Single crystal and powder diffraction studies of the structure of heteropolymolybdophosphoric acid catalysts

B. Herzog, W. Bensch, Th. Ilkenhans, R. Schlögl

Institut für Anorganische Chemie der Universität Frankfurt, Niederurseler Hang, W-6000 Frankfurt 50, Germany

and

N. Deutsch

Central Research, Röhm, GmbH, Kirschenallee, W-6100 Darmstadt, Germany

Received 19 March 1993; accepted 19 April 1993

Single-crystal structures were obtained of several vanadium-substituted forms (with coexistent Cu ions) of heteropolyacid catalysts prepared via hydrothermal synthesis. All V-containing species are of the inverse Keggin type; excessive addition of Cu reverts the structure back to the normal Keggin form. Structural details of the two poly-anions indicate qualitatively different bonding of the bridging oxygen atoms active in catalysis. From the single-crystal data reference powder patterns of the two base structures were simulated and experimentally verified. Failure to observe these patterns in clear form in conventional diffraction experiments is traced back to rapid changes in the state of hydration of the materials, with time constants comparable to acquisition times of powder diffraction data. Thermal dehydration leads to intermediate structures different from those subjected to dehydration in air. The anhydride of $PVMo_{11}$ is stable up to 670 K.

Keywords: Structure–activity relationships; isobutyric acid; methacrylic acid; bifunctional catalysts

1. Introduction

Heteropolyacids [1] (HPA) of the Keggin type [2] are good bifunctional catalysts [3] providing Brønsted acidity and oxygen transfer (redox) functions. The synthesis of methacrylic acid (MAA) from isobutyric acid (IBA) is a particular application in which the bifunctional character of the HPA is fully exploited [4]. The basic catalyst system is $H_4PVMo_{11}O_{40} \cdot 32H_2O$ ($PVMo_{11}$) which provides an active and selective catalyst [5]. Promoters like Cs and Cu were used to increase the

lifetime of the system and to further improve the selectivity [6]. Little is known, however, about the mode of operation of these promoters and the structure of the catalyst under working conditions. Despite the unusual hydrothermal synthesis of the catalyst from insoluble oxides it is generally assumed that the starting catalyst contains the Keggin anion which is obtained in pure form by precipitation [7]. Much more information supporting this assumption is available on the parent heteropolyacid $H_3PMo_{12}O_{40} \cdot XH_2O$ (PMo_{12}) which was investigated as partially deprotonated salt system by several groups showing that under their particular reaction conditions part of the material was of the Keggin structure and part of the material disintegrated to MoO_3 [8]. An advantage of the $PVMo_{11}$ system is the better thermal stability [8] (as compared to the PMo_{12}) thereby allowing a larger content of free acid in the catalyst. The problem of thermal degradation in the present systems is much more severe than in the isostructural heteropolytungstates [9].

To study the exact nature of the catalyst under working conditions we first investigated the structure of the catalyst system. A recent detailed study on the deactivation of $PVMo_{11}$ in selective oxidation of IBA gave evidence for the at least partial disintegration of the HPA without having proof for the existence of the HPA structure under catalytic conditions, i.e. it was clearly found that the system loses Mo but it is not clear from which parent structure [10]. In the present contribution we report single-crystal structure determinations of catalyst materials which were grown from hydrothermal synthesis. In addition, the data were used to construct the powder diffraction patterns of these well characterised reference systems. It is demonstrated that with this information the complex diffraction information obtained from catalyst systems under various conditions can be analysed.

The crystal structures of heteropoly compounds are described [11] in terms of primary structures of the poly-anions and of secondary structures comprising the relative orientation of the anions, the arrangement of the crystal water and the possible formation of microporosity in salt derivatives [12]. Powder X-ray diffraction is sensitive to the secondary structure determining the cell-size and symmetry and is thus a sensitive tool to monitor changes in the hydration and effects of salt-forming cations [13]. (Powder diffraction patterns contain only limited information about the primary structure which dominates the single crystal information as the water molecules are often disordered and contribute only limited scattering power to the whole structure.)

The PMo_{12} primary structure consists of a central tetrahedron PO_4 which determines the molecular symmetry. It is surrounded by four groups of edge-sharing octahedra (M3 triplets) which are interconnected via corners. For the catalytic properties it is important to state that four groups of differently coordinated oxygen atoms with widely varying Mo–O bond lengths exist in the structure, namely four central atoms linking the P atom with the octahedral shell (O_i), 12 terminal Mo–O atoms (O_t) and 24 O atoms in bridging positions in the octahedra which can be divided in one group of 12 atoms within one triplet (O_{b1}) and 12 atoms linking

the triplets with each other (O_{b2}). These bridging atoms were found to be active as oxygen donors [14] reversibly resupplied from gas phase oxygen [15].

The secondary structure of the water-richest form of PMo_{12} can be described as a face-centered-cubic unit cell ($a = 2.3$ nm, $Z = 8$) with each anion being rotated by 90° with respect to each other. The anions are interconnected by bridges of $H_5O_2^+$ units resulting in a non-dense arrangement of the anions with large voids interconnected to a 3D channel system. These channels are filled with the residual water molecules being presented in highly disordered form.

The primary structure of $PVMo_{11}$ was first determined for the PV_2Mo_{10} analogue [16] and found to exhibit an "inverse-Keggin" structure. This anion consists of a disordered PO_4 unit forming on average a cube around which the MoO_6 octahedra form a cubooctahedron. This much more open structure requires highly distorted MoO_6 octahedra with three distinctly different types of oxygen atoms. It is noted that this structure was criticized for the disorder in the central unit by crystallographic arguments and tried to be traced back to a twinned crystal of the normal Keggin structure [17].

The relatively loose packing allows diffusion of polar molecules within the whole bulk of the material and gives potential access to all primary units for catalytic conversion of polar molecules.

For the desired catalytic function the HPA must retain at least partial Brønsted acidity with some protons being neutralized to enhance the thermal stability. Such partially neutralized materials seem, however, not to be single phase but rather be composed of a mixture of free HPA and completely neutralized salts [18].

With this information it is easy to show that the hydrothermal synthesis product is structurally identical to the material described above by powder X-ray diffraction. The stated sensitivity of this method applied under conventional conditions with samples prepared and measured in air does, however, not furnish conclusive and reproducible results. Often very poor patterns [13] or diffractograms with many lines allow no straightforward indexing [19] or preclude even phase analysis by fingerprinting.

2. Experimental

The materials were synthesized hydrothermally from stoichiometric mixtures of metal oxides (MoO_3, V_2O_5, CuO) heated in diluted phosphoric acid. This (industrial) synthesis entails a complicated sequence of reactions, to be described in detail elsewhere. The integrity of all samples was checked by EDX analysis of all single crystals used and by ^{31}P and ^{51}V solid state NMR in addition to conventional chemical analysis and IR spectroscopy (samples as KBr disks). Powder X-ray diffraction was performed on a STOE STADI P instrument (copper or cobalt radiation) equipped with a focussing Guinier transmission goniometer and a 40° position-sensitive detector. Samples were either measured in sealed Lindemann

tubes or, for the dehydration experiments as slurries with mother liquor between X-ray transparent plastic films. Temperature-dependent experiments were performed using a modified Bühler furnace and a reflection goniometer with post-monochromator and a scintillation counter. Temperatures and diffracted angle scales were calibrated using silicon and potassium nitrate as standards. Single crystals were sealed and fixed with paraffin into Lindemann tubes and measured on a STOE AED II 4 circle diffractometer with molybdenum radiation. Relevant details of the structure determinations and data collection are given in the appendices.

3. Results and discussion

The catalytically relevant HPA contain V substituted for Mo, and Cu presumably as cation for partial neutralisation. As both elements influence the catalytic performance we first determined the single-crystal lattice parameters of a variety of materials. In addition, it seemed appropriate to show that conventional alkali salt synthesis and industrial catalyst synthesis lead to the same structures, a problem which could not be solved by powder diffraction. Table 1 reports the results. The data show that the PMo_{12} samples obtained by the hydrothermal synthesis are of the same structure as described in the literature. In addition, the presence of small amounts of copper has no significant influence. All vanadium-containing samples are isomorphic and isostructural to the inverse Keggin type from the literature. The degree of substitution of V for Mo has little systematic influence on the lattice parameters, i.e. there is little chance to structurally determine this catalytically [20] important parameter.

Table 1 further shows that the structures of the vanadium HPA deviate systematically from that of the pure compounds. (It seems rather unlikely that all our crystals should have been twinned only in the presence of vanadium.) Contrary to the crystallographic arguments against the inverse Keggin structure, this present

Table 1
Lattice parameters of HPA catalysts determined from single crystals. All dimensions are given in nm

Sample	Space group	Lattice parameter		
		a	*c*	volume
$H_{2.6}Cu_{0.2}[PMo_{12}O_{40}] \cdot 30H_2O$	Fd-3m	2.330	–	12.7333
$H_2Cu[PVMo_{11}O_{40}] \cdot 30H_2O$	Fd-3m	2.3214	–	12.5098
$H_4[PMo_{12}O_{40}] \cdot 30H_2O$[24]	Fd-3m	2.325	–	n.d.
$H_{3.6}Cu_{0.2}[PVMo_{11}O_{40}] \cdot 32H_2O$	P4/mnc	1.2922	1.8461	3.0826
$H_{4.6}Cu_{0.2}[PV_2Mo_{10}O_{40}] \cdot 32H_2O$	P4/mnc	1.2890	1.8310	3.0482
$H_{5.6}Cu_{0.2}[PV_3Mo_9O_{40}] \cdot 32H_2O$	P4/mnc	1.2870	1.8427	3.0545
$H_5[PV_2Mo_{10}O_{40}] \cdot 30–36H_2O$[16]	P4/mnc	1.2858	1.8341	3.0323

observation is a chemical argument in favour of the existence of the inverse Keggin structure caused possibly by the electron deficiency in the poly-anion resulting from the substitution of Mo (d^4 valence) by V (d^3 valence). For catalytic purposes it is important to estimate the effect of this substitution on the Mo–O bonds as any discernible difference in chemical bonding could lead to an interpretation of the V promoter effect as an electronic modification of the HPA.

The insensitivity of the structural parameters to the extent of substitution of Mo points to the presence of V in a rather similar environment as the Mo is in the parent structure. The irregularities in the lattice parameters further suggest that the samples are microheterogeneous, i.e. despite the macroscopically stoichiometric composition each crystal may contain locally varying degrees of substitution with the X-ray diffraction yielding an average. This was confirmed by a ^{51}V solid state MAS-NMR experiment using single crystals of the nominal composition PV_2Mo_{10}. Fig. 1 shows that at least three different V chemical environments occur in this by X-ray diffraction single-phase material. The resonance at −523 ppm occurs as single line in $PVMo_{11}$ crystals. This means that the PV_2Mo_{10} phase consists of some monosubstituted material, of a main fraction of disubstituted material and to balance the composition of a fraction of higher substituted HPA. Corresponding experiments on even higher substituted samples confirm the trend seen in fig. 1 with an increase in the resonance intensity for "higher substituted" material in parallel to the presence of mono- and disubstituted material. It is noted that all V- containing HPA samples give discrete isotropic chemical shifts despite the non-perfect octahedral symmetry of the chemical environment (see below). In such environments of binary vanadates the resultant spectrum at high field (7 T) is dominated by the chemical shift anisotropy (CSA) and rather complex side band

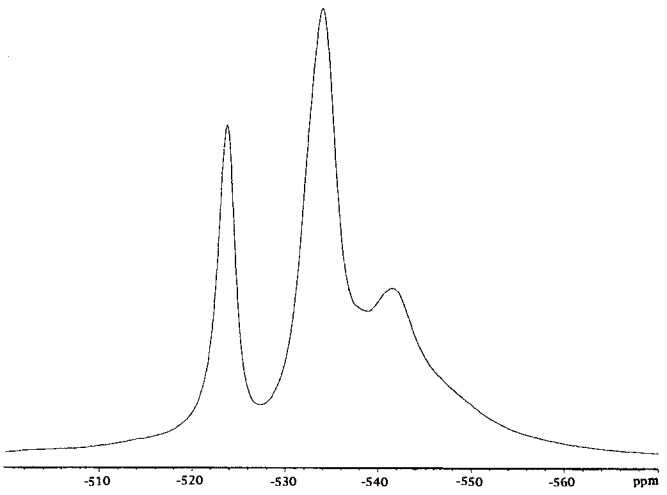

Fig. 1. ^{51}V solid state NMR spectrum of single crystals of $PVMo_{11}$ as 32-hydrate.

patterns should be expected [21]. Possibly, some intramolecular dynamics within the anions averages out the CSA for the ^{51}V NMR.

Detailed single crystal structure analyses were performed with crystals of $H_2Cu[PVMo_{11}O_{40}] \cdot 30H_2O$ and of $H_{3.6}Cu_{0.2}[PVMo_{11}O_{40}] \cdot 32H_2O$. According to previous findings, the same inverse Keggin structure was expected as both crystals contain vanadium (checked by EDX). The sample poor in copper showed the expected structure in agreement with the data in table 1. The copper-rich sample was, however, of the normal Keggin type. This indicates that the cations neutralizing the HPA molecules can also exert a significant influence on the primary structure. Neither the substituted vanadium nor the peripheral copper atoms could be located, however, in the crystal structures. The flatness of the residual difference Fourier synthesis maps of both crystal structures of about 0.9 $e^-/0.001$ nm^3 excludes the localisation even of an only weakly occupied preferred position of the Cu species.

Full descriptions of the crystal structures are in the literature [11,16,17]. Using the present data some details of the structures will be highlighted which are relevant for the catalytic application. In fig. 2 a central section through one normal Keggin unit is shown. The internal PO_4 tetrahedron can be seen clearly. The regular shape of the tetrahedron is a consequence of the local symmetry and not given by chemical reasons. In fact, around the P atom there is residual electron density indicating a slight deviation from the ideal tetrahedron. The MoO_6 octahedra are rather asymmetric with four exactly coplanar bridging oxygens of 0.1901 nm to 0.1905 nm

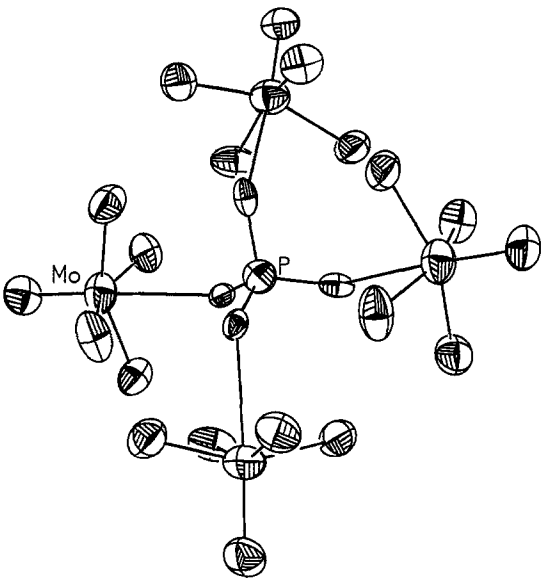

Fig. 2. Section of the Keggin poly-anion showing the connection scheme between the central PO_4 tetrahedron and the MoO_6 octahedra. Details of the asymmetries are described in the text. The displacement elipsoids denote 25% probability radius.

Mo–O bond distances. The O_b–O_b distances vary between 0.2756 nm and 0.2851 nm defining a fairly regular base of the octahedron. One very long Mo–O bond (0.2444 nm) interconnects the octahedron via O_i to the central atom (P–O bond 0.1500 nm). The other apical Mo–O bond to the terminal oxygen O_t is with 0.1679 nm very short. The average of the two apical bonds is close to the planar Mo–O bond distances. The central Mo atom is located 0.043 nm above its ideal position (see bottom octahedron in fig. 2). In summary, the chemical anisotropy of the MoO_6 octahedra can clearly be seen. Only O_b atoms located in the planes of the octahedra can be used for oxygen transfer purposes as the temporal loss of one of these atoms would not seriously destabilize the whole anion; the open O_t atoms are too closely bonded to the central atom and the loosely bonded O_i atoms are inaccessible for exchange purposes. In addition, they seem indispensable for the structural integrity of the whole unit.

The bonding scheme in the inverse Keggin structure is illustrated in fig. 3. The central coordination polyhedron is a cube resulting from a statistical occupation of two orientations of the PO_4 unit. The situation plotted is an average projection as seen by the static X-ray diffraction experiment. The two orientations of the PO_4 units cause a different bonding pattern to the MoO_6 units. Their average structure is now a sevenfold coordinated Mo central atom with the long apical bond split in a fork-like fashion. These forks are present in two orientations relative to the central ligands causing two inequivalent distorted octahedra to exist in the ratio 2 : 1 in the structure. The symmetry of the cube is again determined by the site symmetry

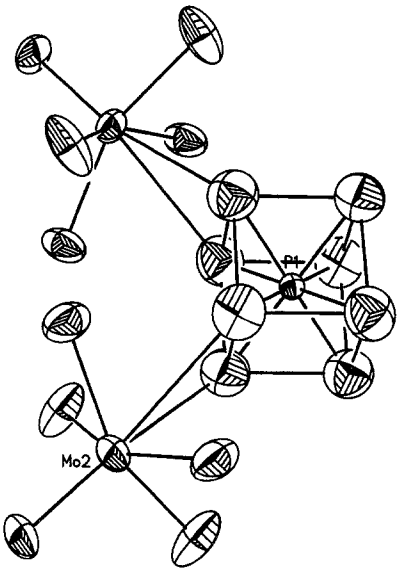

Fig. 3. Section of the inverse Keggin poly-anion showing the connection scheme between the disordered PO_4 group (averaged as a cube) and the distorted MoO_6 octahedra.

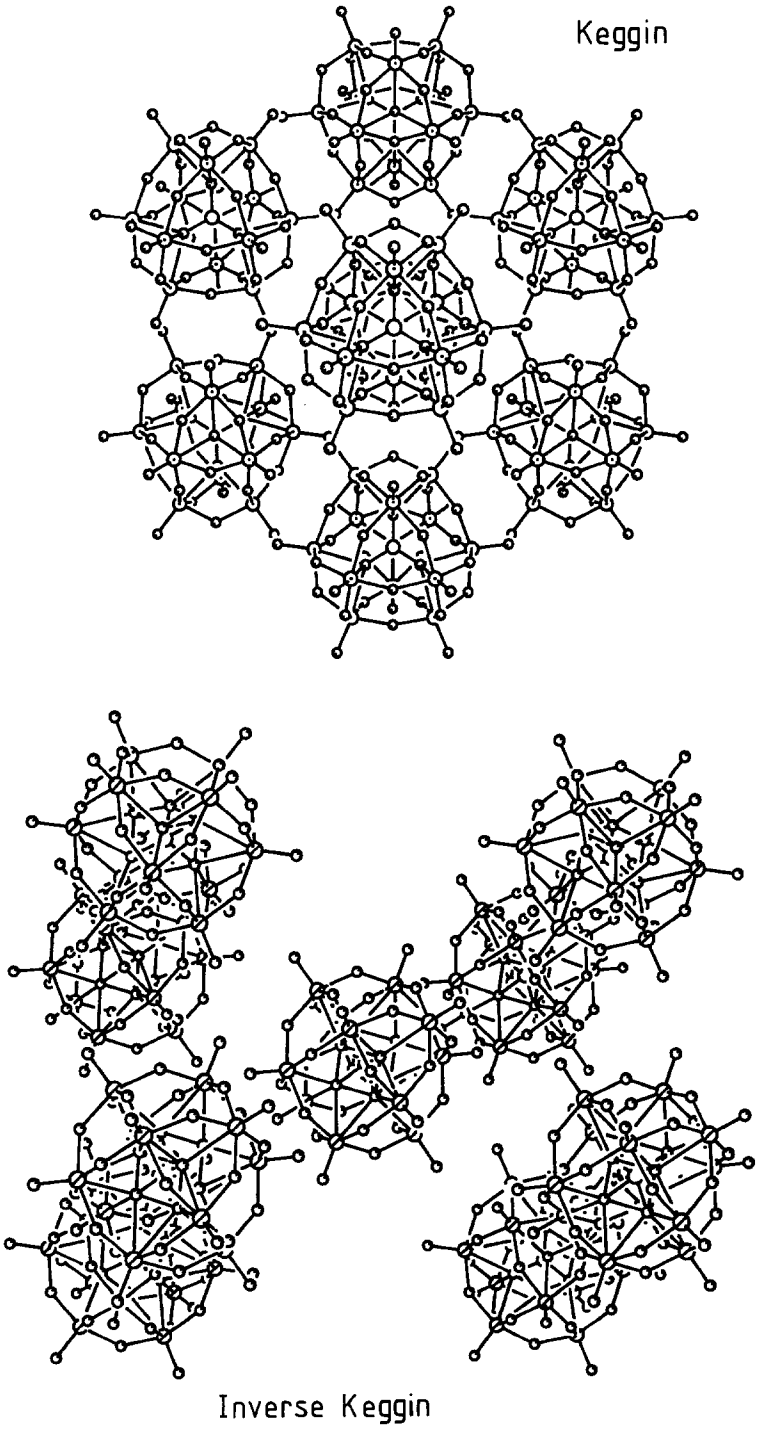

Fig. 4. Packing arrangements of the normal and the inverse Keggin structures.

of the space group; no indication by residual electron density was found for a real lower symmetry of the central polyhedron. The P–O bond (0.154 nm) is longer than in the normal Keggin unit. The Mo–O_b distances (from 0.1886 to 0.1901 nm) are slightly shorter than in the normal Keggin octahedron. The apical short Mo–O_t distance (0.1639 nm) is shorter than in the normal structure. Consequently, the Mo–O_i bond to the central unit is elongated with 0.2469 nm. The bases of the octahedra are even more symmetric than in the normal Keggin unit with a variation in the O_b–O_b bond distances of 0.2743 to 0.2746 nm. The strong deviation of the bonding between the central unit and the shell polyhedra from a regular octahedron justifies a description of the structure as central cube surrounded by 12 edge-sharing quadratic pyramids. The angle between the pyramids within one layer is 91.8°, the angle between pyramids in successive layers is 139.8° so that an elongated cuboctahedron results (see fig. 4) as coordination figure for the whole poly-anion.

In summary, the orientational disorder of the PO_4 unit in the inverse Keggin structure causes a different scheme of connection of the MoO_6 octahedra which in turn leads to slight changes (statistically significant outside the standard deviations of the parameters) in the Mo–O bond distances. One consequence of the two different connection schemes is the different shape of the poly-anions being almost spherical in the normal Keggin structure and more elongated in one direction in the inverse structure. The average diameter approximated by a sphere is rather similar for both units with 1.031 nm for the normal Keggin unit and 1.038 nm for the inverse Keggin anion.

The slight difference in shape of the anions causes a different packing scheme and hence different secondary structures leading to the grossly different lattice parameters of the chemically similar materials. Fig. 4 illustrates this with projections of the unit cells along (111). The different shape of the primary structures is apparent as well as the 90° rotation of the units with respect to each other. The units are interconnected via hydrogen bonding of water molecules placed between the "pins" of outward-directed Mo–O_t bonds. The distance between two "pins" in two anions is 0.3206 nm. The void structures capable of storing additional water or providing channels for diffusion of polar molecules can also be recognised.

In fig. 5 a larger portion of the packing of the $PVMo_{11}$ structure is displayed. In this (100) projection the "surface" of the material being formed by the strongly bonded O_t species is clearly recognised. These oxygens provide sites for anchoring substrate molecules via hydrogen bonding. The channel structure of the solid is clearly visible allowing all primary units to participate in catalytic action on small molecules.

In summary, from the single crystal structures of PMo_{12} and $PVMo_{11}$ there is no evidence for a significant effect of either V or Cu promotion on the Mo–O bond distances. One consequence of the disorder in the central PO_4 unit leading to the inverse Keggin structure is a modification of the Mo–Mo distances: the normal Keggin structure is composed of four triplets of octahedra in which the Mo–Mo distances are 0.340 nm. The Mo–Mo distances between corner-sharing octahedra

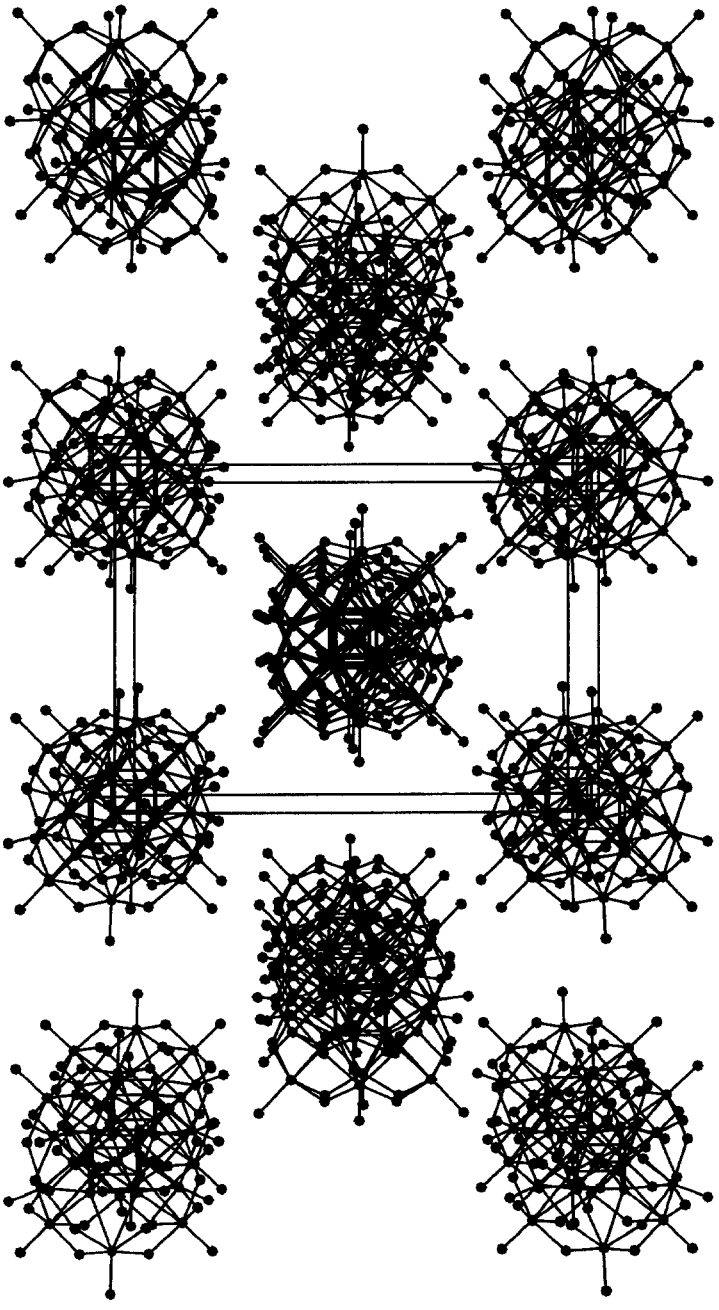

Fig. 5. Expansion of the packing scheme of the inverse Keggin structure. The central frame indicates the unit cell shown in fig. 4.

occurring at the links of the triplets are elongated to 0.370 nm. In the inverse Keggin structure no grouping to triplets occurs with the consequence that only one Mo–Mo distance is observed of 0.390 nm. In addition, the Mo–O_i bond is qualitatively different in the two structures: in the normal Keggin unit the bond direction is perpendicular to the base of the octahedron (see fig. 2) and thus in line with the d-orbital direction. In the inverse structure the fork-like bonding causes an angle between the central plane of the octahedron and the O_i bond of about 70° representing a significant "misalignment" of this bond with respect to the d-orbital direction. If the suggestion of significant covalent bonding in the HPA anions [22] is followed, these geometric differences may have implications on the bond strengths of the catalytically important Mo–O_b bonds and thus on the oxygen transfer activity of the two types of HPA anions: the bond angles Mo–O_b–Mo are 138.9° in the inverse structure and 152.1°/126.7° in the normal Keggin structure. However, the structural information is an average bulk information and cannot contribute information about the local chemical environment of the V substituted M–O_6 octahedra.

To approach the nature of the active phase of the $PVMo_{11}$ catalyst under reaction conditions an in situ powder diffraction experiment has to be performed requiring detailed knowledge of the diffraction pattern of the verified $PVMo_{11}$

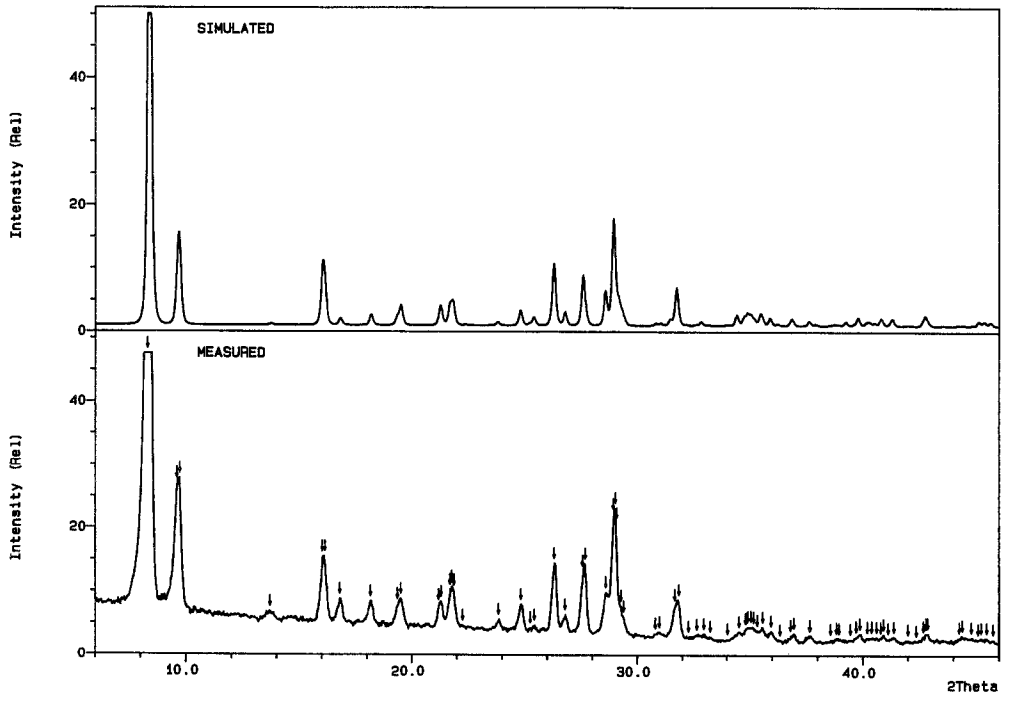

Fig. 6. Powder diffraction pattern (Cu radiation) of $PVMo_{11}$ in the 32-hydrate form. The top trace is the simulation from the single crystal data, the bottom trace represents an experimental pattern.

material. Using the experiences in preparing single crystals of the material and calculating the theoretical powder diffraction pattern from the single crystal structural data it was possible to obtain the patterns in fig. 6. The top trace shows the theoretical powder pattern of $PVMo_{11}$ as 32-hydrate whereas the lower trace represents the experimentally measured pattern. The agreement is excellent and allows to use this pattern as reference in further structural work. The same procedure was carried out with the normal Keggin structure leading to the same good agreement with experiment and also to a theoretical pattern derived from a crystal structure [22] of pure PMo_{12}. This agreement shows that powder X-ray diffraction alone is inadequate to characterize the substitutional status of the HPA catalysts used in the MMA synthesis. Table 2 lists the principal indexed diffraction lines for both phases.

Powder diffraction of catalyst materials measured dry in air often yield diffuse patterns which are difficult to index or indicate the presence of more than one phase. This is not due to an intrinsic ill-defined catalyst but occurs as an artifact from dehydration during data acquisition. The phenomenon was followed with $PVMo_{11}$ in a time-resolved diffraction experiment the result of which is displayed in fig. 7. The group of reflections at low angles is indicative for the change in the secondary structure and shows by its initial increase in intensity a crystallisation process (in the mother liquor) followed after about 50 min by a gradual phase change over ca. 125 min (splittings, loss of intensity) into a stable form persisting for several further hours. The whole change is due only to a loss of water as was

Table 2
Calculated powder diffraction data for PMo_{12} and $PVMo_{11}$ samples in their highest hydrate forms. Only reflections with significant intensities are given

$PVMo_{11}$			PMo_{12}		
d-spacing	*hkl*	int.	*d*-spacing	*hkl*	int.
10.528	101	100	13.226	111	100.0
9.170	002	6.8	8.221	220	9.1
9.091	110	10.8	5.335	331	1.1
5.521	103	8.6	4.475	333	3.8
5.486	211	4.1	4.110	440	1.0
3.385	313	9.8	3.546	533	2.1
3.228	224	7.8	3.356	444	8.0
3.118	410	5.3	3.256	711	1.0
3.080	323	15.2	3.027	533	3.6
2.815	324	6.0	2.906	800	2.1
			2.685	555	1.9
			2.552	911	1.4
			2.478	664	1.8
			2.337	755	1.4
			2.280	862	1.0

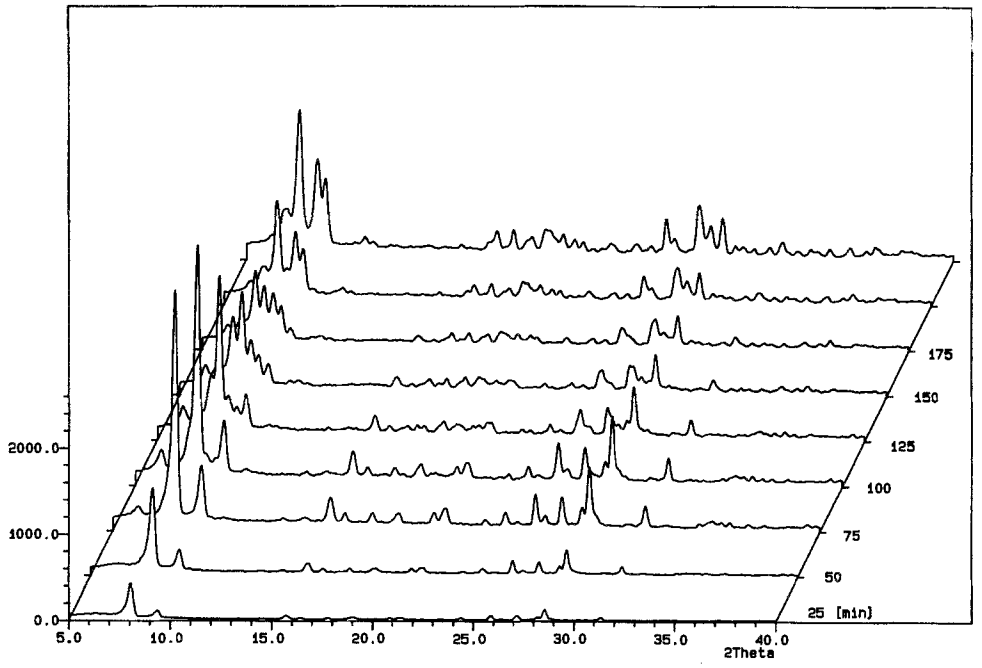

Fig. 7. Time-resolved powder diffraction data (Cu K_α, focussed geometry) of the 32-hydrate of $PVMo_{11}$. Successive scans were recorded every 25 min with the sample kept at 300 K between plastic foils in air without a gas stream.

shown by a linear correlation between the weight change of the material in air and the intensity change of characteristic reflections for the 32-hydrate phase of $PVMo_{11}$. The weight loss is featureless and converges to a value of hydration of about 24 moles water in agreement with literature [7] data (24–25 moles). The dehydration process is complicated as follows from a plot of the total integrated intensity of the diffraction patterns as function of time: a pronounced minimum at maximum conversion rates indicates an X-ray amorphous intermediate state of the sample. The experiment yields as second reference diffraction pattern that of the 24-hydrate which can also be obtained quickly and reproducibly by warming the sample in air to 330 K.

Further drying at 300 K in vacuo or over H_2SO_4 leads to new patterns very rich in lines. The next lower 14-hydrate is indeed a triclinic structure [19] the simulation of which from published single crystal data [23] agreed well with our experimental observation and a previous simulation in the literature [8]. It is noteworthy that the diffraction patterns of strongly dehydrated PMo_{12} and $PVMo_{11}$ materials become more and more similar to each other. This analytical difficulty is caused by the fact that after excessive dehydration the secondary structures of the HPA become progressively more similar as they approach the closest possible packing of the polyanions.

Higher substitution of Mo by V significantly stabilizes the compounds against dehydration in air. The $PV_2Mo_{10}O_{40}$ phase in its 32-hydrate form is stable for over 200 min in air before detectable dehydration sets in which is finished after 24 h at the level of an about 27-hydrate. The corresponding diffraction patterns are almost unchanged in their lattice parameters. The two additional acid functions caused by the substitution increase the "stiffness" of the framework of the secondary structure (see figs. 4, 5) such that partial loss of water molecules does not significantly shrink the unit cell.

The dehydration process leads to different products if simultaneously heating and a dry nitrogen stream are applied. The heating cycle of such an experiment with $PVMo_{11}$ material is shown in fig. 8. The nitrogen stream converts the 32-hydrate at 300 K immediately into the 24-hydrate giving rise to the first pattern. At 330 K we observed the 6-hydrate phase without going through the stage of the 14-hydrate. The following patterns are all characteristic of the anhydride: this poorly crystalline material is reversibly converted to the 24-hydrate upon cooling in air to 300 K. The final sharp pattern is observed after heating to 700 K and represents MoO_3: this conversion is irreversible. No other phases of vanadium or copper oxides or mixed compounds can be identified. Similar but less complete data are reported in the literature [19] in film experiments with the sample held in moist air.

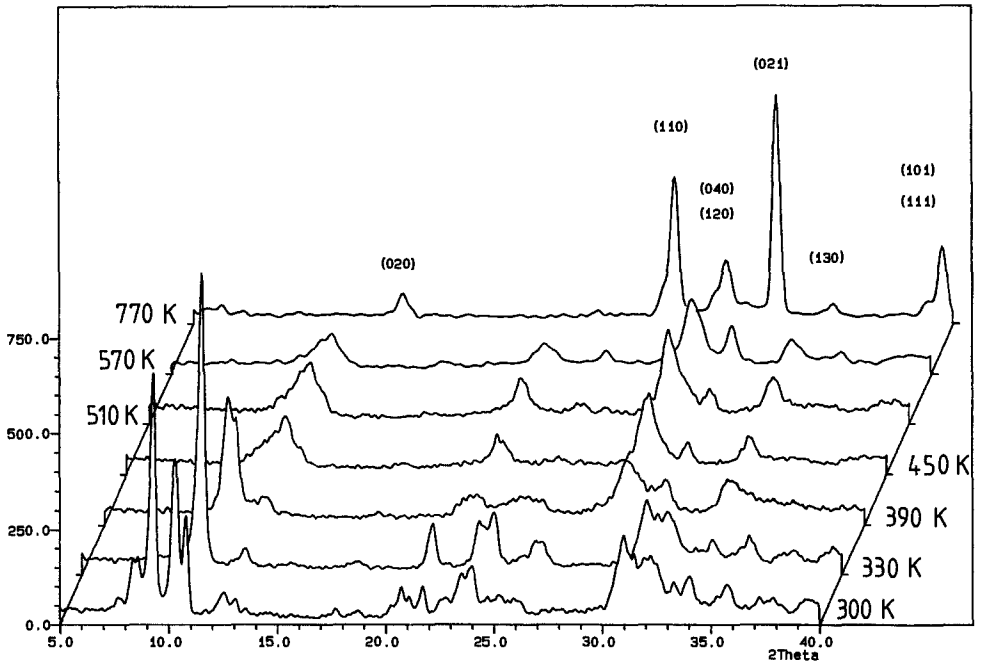

Fig. 8. Temperature-dependent powder diffraction data of $PVMo_{11}$ (Co K_α, reflection geometry). Data recorded under flowing nitrogen. The indexing for the last trace denotes the reflections of MoO_3.

4. Conclusions

In search for the structural identity of the HPA catalysts used in the conversion of IBA to MAA a number of structure determinations with different diffraction techniques under various conditions were carried out allowing to state the following points.

The industrial hydrothermal synthesis of catalysts produces the same structures as the conventional alkaline salt synthesis route.

Substitution of Mo by V causes a disorder in the Keggin structure leading to the inverse Keggin structural motif.

Addition of stoichiometric amounts of Cu reverts the structure in the presence of V back to the normal Keggin type.

The degree of substitution of Mo by V and the phase purity cannot be determined by X-ray diffraction. Substitution in excess of 1 V per poly-anion leads to phase-mixed products as identified by ^{51}V solid state NMR.

Neither Cu nor V can be localized in the structures by X-ray diffraction.

Different connection schemes in the two types of poly-anion structures lead to rather similar Mo–O bond lengths but significantly different Mo–O_b–Mo bond angles which may have implications on the oxygen transfer activities of the two poly-anion types. The packing of both primary structures is different due to small modifications in the shape of the units. In both structures the surfaces of the poly-anions are determined by pin-like Mo–O_t bonds keeping the units from forming close-packed structures and allowing the water molecules to form a labile framework of secondary structures depending in their dimensions on the extent of hydration. In the maximum hydrated state the channels are wide enough to permit polar molecules to penetrate into the bulk of the material and to potentially utilize catalytically all primary units.

Well-defined powder diffraction reference patterns are now available for phase identification. Conventional powder diffraction in air is difficult to analyse due to a rapid de- or rehydration of extreme hydration states to an average state with time constants similar to typical acquisition times of diffraction experiments. First in situ diffraction data indicate that both, temperature and gas conditions influence the pathway of dehydration. A temperature stability limit of 570 K was found for the $PVMo_{11}$ phase after which irreversible disintegration to MoO_3 occurred. Higher degrees of substitution render the samples less susceptible to dehydration at 300 K. In highly dehydrated samples discrimination between PMo_{12} and $PVMo_{11}$ materials becomes difficult by powder diffraction.

This information indicates that such catalysts can only be characterised structurally under in situ conditions and additional information about their chemical compositions is mandatory for a phase analysis. In addition, the data will allow the analysis of diffraction experiments under reaction conditions currently being done. The structural details now available may stimulate further work to elucidate the mode of operation of these versatile catalytic chemicals.

Acknowledgement

The work was conducted in cooperation with RÖHM GmbH (Darmstadt). We acknowledge efficient and friendly collaboration with Th. Haeberle, E. Bielmeier, H. Siegert and G. Emig (University of Karlsruhe). Financial support came also from the Fonds der Chemischen Industrie and from the Röhm Foundation.

Appendices

Appendix 1. Details of the single crystal structure determination of the normal Keggin sample $H_{2.6}Cu_{0.2}[PMo_{12}O_{40}] \cdot 30H_2O$.

lattice parameters (Å)	23.214(3)	R_{int} (%)	2.82
space group	Fd-3m	$N_0(F_0 > 4.0\sigma(F_0))$	291
volume (Å^3)	12510(3)	N_p	34
Z	8	min. transmission	0.5628
MG	1918.3	max. transmission	0.7617
Dcalc (Mg/m^3)	2.037	y^a	0.001
absorption coeff. (mm^{-1})	2.369	R(%)	6.41
F(000)	7096	Rw(%)	6.18
$2\Theta°$	3.0–50.0	GOF	1.85
$\sum I$	1572	δ(e/Å^3)	1.00
unique data	576		−0.76

[a] In weighting scheme $w = 1/[\sigma^2(F) + yF^2]$.

Appendix 2. Details of the single crystal structure determination of the inverse Keggin sample $H_{3.6}Cu_{0.2}[PVMo_{11}O_{40}] \cdot 32H_2O$.

Bond lengths (Å)

Mo(1)–O(2)	1.639(6)	Mo(1)–O(3)	1.889(7)
Mo(1)–O(4)	1.898(8)	Mo(1)–O(5)	1.901(7)
Mo(1)–O(5)	1.893(7)	Mo(1)–O(7)	2.468(8)
Mo(1)–O(7)	2.459(9)		
Mo(2)–O(1)	1.648(8)	Mo(2)–O(3)	1.896(7)
Mo(2)–O(4)	1.887(7)	Mo(2)–O(7)	2.469(9)
Mo(2)–O(3B)	1.896(7)	Mo(2)–O(4A)	1.887(7)
Mo(2)–O(7D)	2.469(9)		
P(1)–O(7A)	1.530(9)		

Bond angles (deg)

O(2)–Mo(1)–O(3)	102.0(3)	O(2)–Mo(1)–O(4)	101.5(3)
O(3)–Mo(1)–O(4)	87.5(3)	O(2)–Mo(1)–O(5)	101.1(3)
O(3)–Mo(1)–O(5)	156.9(3)	O(4)–Mo(1)–O(5)	86.9(3)
O(2)–Mo(1)–O(5)	101.9(3)	O(3)–Mo(1)–O(5)	88.0(3)
O(4)–Mo(1)–O(5)	156.7(3)	O(5)–Mo(1)–O(5)	88.3(4)
O(2)–Mo(1)–O(7)	159.5(3)	O(3)–Mo(1)–O(7)	64.3(3)
O(4)–Mo(1)–O(7)	93.3(3)	O(5)–Mo(1)–O(7)	93.7(3)

O(5)–Mo(1)–O(7)	64.2(3)	O(2)–Mo(1)–O(7)	158.5(3)
O(3)–Mo(1)–O(7)	93.1(3)	O(4)–Mo(1)–O(7)	63.7(3)
O(5)–Mo(1)–O(7)	64.3(3)	O(5)–Mo(1)–O(7)	93.7(3)
O(7)–Mo(1)–O(7)	42.0(4)		
O(1)–Mo(2)–O(3)	101.1(3)	O(1)–Mo(2)–O(4)	102.7(3)
O(3)–Mo(2)–O(4)	87.8(3)	O(1)–Mo(2)–O(7)	159.0(2)
O(3)–Mo(2)–O(7)	93.3(3)	O(4)–Mo(2)–O(7)	93.0(3)
O(1)–Mo(2)–O(3)	101.1(3)	O(3)–Mo(2)–O(3)	86.9(4)
O(4)–Mo(2)–O(3)	156.2(3)	O(7)–Mo(2)–O(3)	64.2(3)
O(1)–Mo(2)–O(4)	102.7(3)	O(3)–Mo(2)–O(4)	156.2(3)
O(4)–Mo(2)–O(4)	87.9(4)	O(7)–Mo(2)–O(4)	63.6(3)
O(3)–Mo(2)–O(4)	87.8(3)	O(1)–Mo(2)–O(7)	159.0(2)
O(3)–Mo(2)–O(7)	64.2(3)	O(4)–Mo(2)–O(7)	63.6(3)
O(7)–Mo(2)–O(7)	42.0(4)	O(3)–Mo(2)–O(7)	93.3(3)
O(4)–Mo(2)–O(7)	93.0(3)		
O(7)–P(1)–O(7)	180.0(1)	O(7)–P(1)–O(7)	109.3(6)
O(7)–P(1)–O(7)	70.7(6)		

References

[1] M.T. Pope and A. Müller, Angew. Chem. 103 (1991) 56.
[2] J.F. Keggin, Proc. Roy. Soc. A 144 (1934) 75.
[3] M. Misono, Catal. Rev.-Sci. Eng. 29 (1987) 269.
[4] M. Otake and T. Onoda, in: *Proc. 7th Int. Congr. on Catalysis*, Tokyo 1980, eds. T.S. Seiyama and K. Tanabe (1981) p. 780.
[5] T. Haeberle and G. Emig, Chem. Ing. Technol. 2 (1988) 392.
[6] M. Ai, J. Catal. 85 (1984) 324.
[7] G.A. Tsigdinos and C.J. Hallada, Inorg. Chem. 7 (1968) 437.
[8] J.B. Black, N.Y. Clayden, P.L. Gai, J.D. Scott, E.M. Serwicka and J.B. Goodenough, J. Catal. 106 (1987) 1;
J.B. Goodenough, Solid State Ionics 26 (1988) 87.
[9] H. Hayashi and J.B. Moffat, J. Catal. 77 (1982) 473.
[10] O. Watzenberger, G. Emig and D.T. Lynch, J. Catal. 124 (1990) 247.
[11] H.T. Evans, Perspec. Struct. Chem. 5 (1971) 1.
[12] G.B. McGarvey and J.B. Moffat, J. Colloid Interf. Anal. 125 (1988) 473.
[13] G.B. McGarvey and J.B. Moffat, Catal. Lett. 16 (1992) 173.
[14] K. Eguchi, Y. Toyozawa, N. Yamazone and T. Sejima, J. Catal. 83 (1983) 32.
[15] M. Akimoto, Y. Tsuchida, K. Sato and E. Echigoya, J. Catal. 72 (1981) 83.
[16] V.A. Sergienko, M.A. Korai-Koshits and E.N. Youchenko, J. Struct. Chem. 21 (1980) 87.
[17] H.T. Evans and M.T. Pope, Inorg. Chem. 23 (1984) 501.
[18] E.M. Serwicka, J.B. Black and J.B. Goodenough, J. Catal. 106 (1987) 23.
[19] H.G. Jerschkewitz, E. Alsdorf, H. Fichtner, W. Hanke, K. Jancke and G. Öhlmann, Z. Anorg. Allg. Chem. 526 (1985) 73.
[20] G. Emig, A. Schraut and H. Siegert, Chem. Ing. Tech. 60 (1988) 1061.
[21] H. Eckert and I.E. Wachs, Mater. Res. Soc. Symp. Proc. 11 (1989) 459.
[22] K. Eguchi, T. Seiyama, N. Yamazoe, S. Kutsuki and H. Taketa, J. Catal. 111 (1988) 336.
[23] H. Damour and R. Allmann, Z. Krist. 143 (1976) 1.
[24] J.C. Clark and D. Hall, Acta Cryst. B 32 (1976) 1545.